Diurnal Behavior of Near-surface Aerosols Investigated Using a Near Horizontal Lidar

Prane Mariel Ong[1, 2], Nofel Lagrosas[2], Tatsuo Shiina[1], Hiroaki Kuze[1,2]

[1]*Chiba University, 1-33 Yayoi-cho, Inage-ku, Chiba, 263-8522, Japan*

[2]*Center for Environmental Remote Sensing (CEReS), Chiba University,*

1-33 Yayoi-ku, Inage-ku, Chiba 263-8522, Japan

*Email: prane.ong@chiba-u.jp

Abstract: Studying near-surface aerosols is of importance in improving the assessment of the effect of aerosol radiative forcing to climate. We investigate the diurnal behavior of aerosol extinction coefficients and single scattering albedo (SSA) at 349 nm in relation to the variation of relative humidity under clear-sky, cloudy, and rainy conditions. It is found that the aerosol growth during the condensation phase of water vapor is more readily observed than in the evaporation phase, and the SSA tends to decrease from 50-70% RH during the condensation phase of water vapor due to increase in the influence of elemental black carbon.

Key Words: Lidar, Aerosol Extinction, Single Scattering Albedo, Relative Humidity

1. Introduction

Aerosol plays a vital role in the Earth climate change[1]. One parameter that controls visual air quality is the aerosol extinction coefficient. Lidar studies have elucidated aerosol and cloud behavior at relatively higher altitudes, but studies in the near-surface range are still lacking. In this paper, we examine the diurnal variation of aerosol extinction coefficient, α_{Ext}, and single scattering albedo (SSA) by focusing on the lower troposphere where most of the sources and sinks of aerosol are located. The values of α_{Ext} are derived from a near-horizontal lidar system. Then, they are related to the diurnal pattern of the relative humidity (RH) to examine the possibility of detecting variation in aerosol size distribution due to hygroscopic behavior.

2. Instruments and Methodology

A campaign was conducted for the month of November 2017 using a near-horizontal lidar, an aethalometer and a weather monitor to investigate the diurnal variation of near-surface aerosol extinction (α_{Ext}) and SSA with RH over various sky conditions.

The instruments are located on the rooftop of an eight-story building (~45 m above the ground) in Chiba University in Japan (35.62°N, 140.10°E). The campus is in the urban area of Chiba City, along the east side (~4 km away) of the Tokyo Bay.

The near-horizontal lidar system, as shown in Fig. 1, is pointed in the direction of 10° east of north with an elevation angle of ~2°. The direction is so chosen to minimize the influence of direct solar radiation. Although the system is originally a plan position indicator (PPI) lidar that can perform 360° azimuthal rotation[2], it was operated in a static mode during this campaign, recording data every 5 min continuously. The lidar is based on a diode-laser pumped Nd:YLF laser emitting at 349 nm wavelength with 60 μJ pulse energy and 1 kHz pulse repetition frequency. A photomultiplier tube (PMT, Hamamatsu H10304-00-NN) is used as the receiver sensor. The PMT is connected to a transient
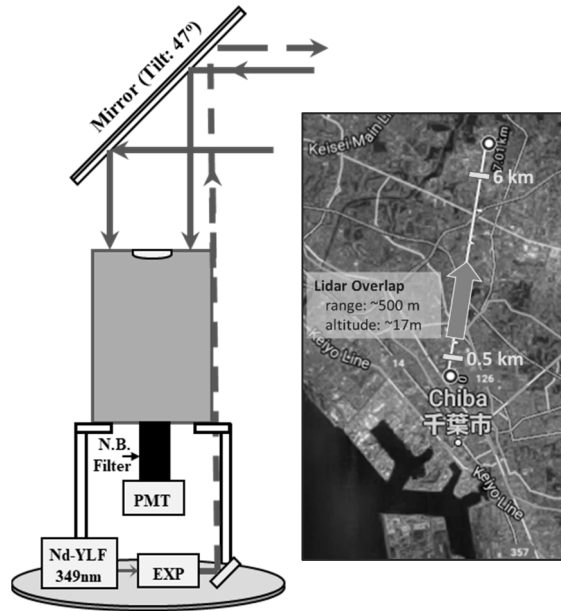

Fig. 1. Schematic diagram of the lidar system with inset google map of the experiment site. Map source (retrieved: April 1, 2019): *https://www.google.com/maps/@35.6325731,140.138 7914,21913m/data=!3m1!1e3.*

recorder (Licel, TR20-160) for data recording of the backscattered signal with 7.5 m range resolution. The obtained data are used to calculate the aerosol extinction coefficient (α_{Ext}) using the Klett method and adaptive slope method[3–5]. Klett Method is an inversion solution to the lidar backscattered signal expressed as

$$\alpha_{Ext}(R) = \frac{X(R)}{\frac{X(Rmax)}{\alpha_{Ext}(Rmax)} + 2\int_R^{Rmax} X(R)dR}. \quad (1)$$

Here $X(R)$ is the range corrected lidar return signal, which is dependent on the range, R. R_{max} is the maximum observable range or the range at the boundary condition. As for the value of $\alpha_{Ext}(R_{max})$ needed as input parameter in Eq. (1), we employ the adaptive slope method of Pan *et al.*[5] These methods are used on the premise that a

well-mixed layer of aerosol exists below the maximum covered altitude of 200 m (at ~6 km range).

A seven-wavelength (370, 470, 520, 590, 660, 880, 950 nm) aethalometer (Magee, AE31) is also utilized to observe the absorptive property of particles. Specifically, it measures the elemental black carbon (EBC) concentration, which then is used to estimate the absorption coefficient (α_{Abs}) as

$$\alpha_{Abs} = (EBC * 10^{-9}) * \left(\frac{6834}{\lambda}\right). \qquad (2)$$

Here λ is the wavelength in nm. To be parallel with the lidar wavelength at 349 nm, extrapolation of α_{Abs} at 370, 470 and 520 nm was done as it changes with time. This derived α_{Abs} at 349 nm, was then used to calculate the SSA given the $\alpha_{Ext}(Alt$: 17 m) from lidar as

$$SSA = \frac{\alpha_{Scat}}{\alpha_{Ext}}. \qquad (3)$$

The maximum value of SSA is unity, which indicates pure scattering, while the value less than one represents the contribution of absorption in the light extinction.

The site is also equipped with a weather monitor (Davis, Vantage Pro 2) that constantly measures the ambient weather parameters including temperature, RH, rain rate, wind speed and direction every 5 min.

3. Results and Discussion

Figure 1 shows the diurnal variation (1-day cycle) of α_{Ext} and SSA with respect to increasing RH (condensation phase of water vapor) and decreasing RH (evaporation phase of water vapor) in clear sky condition observed on November 5, 2017. In order to categorize sky conditions (clear, cloudy, and rainy), we utilized the sunphotometer direct solar radiation data (daytime only). The typical diurnal pattern of RH for the whole campaign is midday minimum (condensation phase onset) and late evening high (evaporation phase onset). Under relatively weak wind speeds (<5 ms^{-1}), the aerosol optical property (α_{Ext} and SSA) is thought to be controlled mainly by the effect of increasing/decreasing RH. For the selected day of November 5, the wind speed was less than 3 m·s^{-1} and the wind came from either N-NE (urban aerosols) or S (maritime aerosol) directions, but mostly from N-NE directions.

Most aerosols are relatively in a dry state at a very low RH (~30%), and condensation of water vapor influences
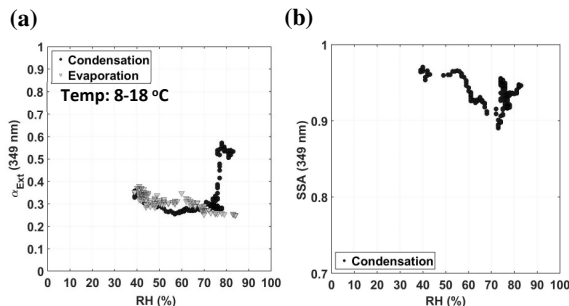
their growth, and because of this growth, they generally scatter more light[7,8]. From Fig. 2a, we can see that during the condensation phase of water vapor the curve pattern of α_{Ext} is comparable to Fig. 1. of Rood et al.[9], where the growth of $(NH_4)SO_4$ in a phase transformation curve as a function of RH was presented. Similarly, as the RH increases (38%<RH<75%) the value of α_{Ext} is almost constant in time, and at the deliquescence humidity (~75% RH) the sudden increase in α_{Ext} occurs. The evaporation phase of water vapor, on the other hand, is seen typically around early dawn to midday (with temperature of about 8-18 °C), but the hysteresis is not that observable.

In Fig. 2b, it is interesting to note that there is a decrease of SSA (more influence from light absorption) during the early stage of the condensation phase of water vapor (40%>RH>70%) then increase again for RH>70%. During this decrease in SSA, we validated the increase on the number of EBC count, which can influence light absorption. Unfortunately for the selected day, there is no data from the aethalometer during the evaporation phase so further analysis cannot be done.

3. Summary

In this paper, we presented the effect of the relative humidity in the aerosol extinction coefficient and single scattering albedo using a near-horizontal lidar system operated at 349 nm. Moreover, the aerosol growth during the condensation phase of water vapor is more clearly observed than in the evaporation phase. The SSA tends to have a dip at 50-70% RH due to increase in EBC count.

References

1. IPCC. *In: Climate change 2007: the physical science basis.* (2007).
2. Mabuchi, Y. *et al.* Multi-wavelength lidar system for the characterization of tropospheric aerosols and clouds. *Int. Geosci. Remote Sens. Symp.* 2505–2508 (2012). doi:10.1109/IGARSS.2012.6351839
3. Klett, J. D. Stable analytical inversion solution for processing lidar returns. *Appl. Opt.* **20**, 211 (1981).
4. Klett, J. D. Lidar calibration and extinction coefficients. *Appl. Opt.* **22**, 514–515 (1983).
5. Klett, J. D. Lidar inversion with variable backscatter/extinction ratios. *Appl. Opt.* **24**, 1638–1643 (1985).
6. Pan, Y.-B., Lu, D.-R., and Pan, W. A New Method for Aerosol Retrieval Based on Lidar Observations in Beijing. *Atmos. Ocean. Sci. Lett.* **7**, 203–209 (2014).
7. Toon, O. B. & Pollack, J. B. A Global Average Model of Atmospheric Aerosols for Radiative Transfer Calculations. *Journal of Applied Meteorology* **15**, 225–246 (1976).
8. Sloane, C. S. Optical properties of aerosols of mixed composition. *Atmos. Environ.* **18**, 871–878 (1984).
9. Rood, M. J., Shaw, M. A., Larson, T. V. & Covert, D. S. E -. *Nature* **337**, 537–539 (1989).

(a)   (b)

Fig. 2. Diurnal variation (1-day cycle) of the α_{Ext} and SSA with respect to RH in clear sky condition.